New on-fault evidence for a great earthquake in A.D. 1717, central Alpine fault, New Zealand

G.P. De Pascale[1]* and R.M. Langridge[2]

[1]Department of Geological Sciences, University of Canterbury, Private Bag 4800, Christchurch, New Zealand
[2]GNS Science, PO Box 30-368, Lower Hutt, New Zealand

ABSTRACT

The dextral-reverse Alpine fault is the major onshore plate-boundary structure between the Australian and Pacific plates in New Zealand. No previous study of the central portion of the 200-km-long central segment has provided on-fault evidence for the most recent event (MRE). Using lidar (light detection and ranging) data coupled with field mapping, we recognized the main trace of the Alpine fault north of Gaunt Creek (South Island) as a north-striking fault scarp. We enhanced a natural exposure that revealed evidence for repeated late Holocene thrust fault movement. The north-northwest–striking fault zone is characterized by a distinct 5–50-cm-thick clay fault-gouge layer juxtaposing hanging-wall bedrock (mylonites and cataclasites) over unconsolidated late Holocene footwall colluvium. The bedrock is cut by a strath terrace and overlain by mid-Holocene (ca. 5400 calibrated ^{14}C yr B.P.) alluvial terrace, which has been faulted repeatedly and is conformably overlain by undeformed late Holocene colluvium and alluvium. An unfaulted peat at the base of the scarp is buried by post-MRE alluvium and yields a calibrated 2σ radiocarbon age of A.D. 1710–1930, which dates the MRE as post-1709. Our data are consistent with sparse on-fault data, and validate earlier off-fault records that suggest an A.D. 1717 MRE. The 1717 event had a moment magnitude of M_w 8.1 ± 0.1, based on the 380-km-long surface rupture. Because the fault has not ruptured for ~300 yr, it is likely approaching the end of its seismic cycle and poses a significant seismic hazard to New Zealand.

INTRODUCTION

The Alpine fault is a major dextral-reverse fault that accommodates much of the motion between the Pacific and Australian plates (Fig. 1) along the western side of the South Island of New Zealand (Wellman, 1953). The fault accommodates 50%–80% of the 37 ± 2 mm yr^{-1} of motion across the plate boundary (Berryman et al., 1992; DeMets et al., 1994; Sutherland et al., 2006) and is estimated to rupture in large to great earthquakes (Sutherland et al., 2007), but has not ruptured during the short historical period in New Zealand (since 1840). An alternative hypothesis (Walcott, 1978) suggests that aseismic creep accommodates the majority of the plate-boundary motion. Based on lichenometric dating of coseismic rock falls (Bull, 1996), post-earthquake aggradational terraces (Adams, 1980), paleoseismic trenching along the fault at the northern terminus of the central section, tree-ring dating studies (Wells et al., 1999), deformed river terraces, buried surfaces, fallen trees (Adams, 1980; Yetton, 2000), and coastal dune progradation sequences (Wells and Goff, 2007), the most recent event (MRE) occurred ca. A.D. 1717; it is possible that earlier ruptures occurred ca. 1615, ca. 1430, and ca. 1230. Dendrochronology shows the highest temporal resolution for the MRE along the fault with abrupt tree growth decline due to earthquake damage along the fault in 1717 (Wells et al., 1999). Based on these studies, the fault is considered near the end of its current earthquake cycle (Sutherland et al., 2007); there is an estimated probability of 30% for a large earthquake in the next 50 yr (Rhoades and Van Dissen, 2003). Although 2 large earthquakes in Canterbury of M_w 7.1 and M_w 6.3 in 2010 and 2011 caused extensive damage and liquefaction (e.g., Cubrinovski et al., 2011; Quigley et al., 2012), the higher magnitude potential from Alpine fault earthquakes makes it the greatest seismic hazard for the South Island (Fig. 2).

On geomorphic and structural grounds the typically linear Alpine fault (when viewed at small scales; e.g., satellite imagery, 1:100,000 topographic maps) is generally divided into the southern, central, and northern sections (Fig. 3). The late Quaternary geological dextral slip rates

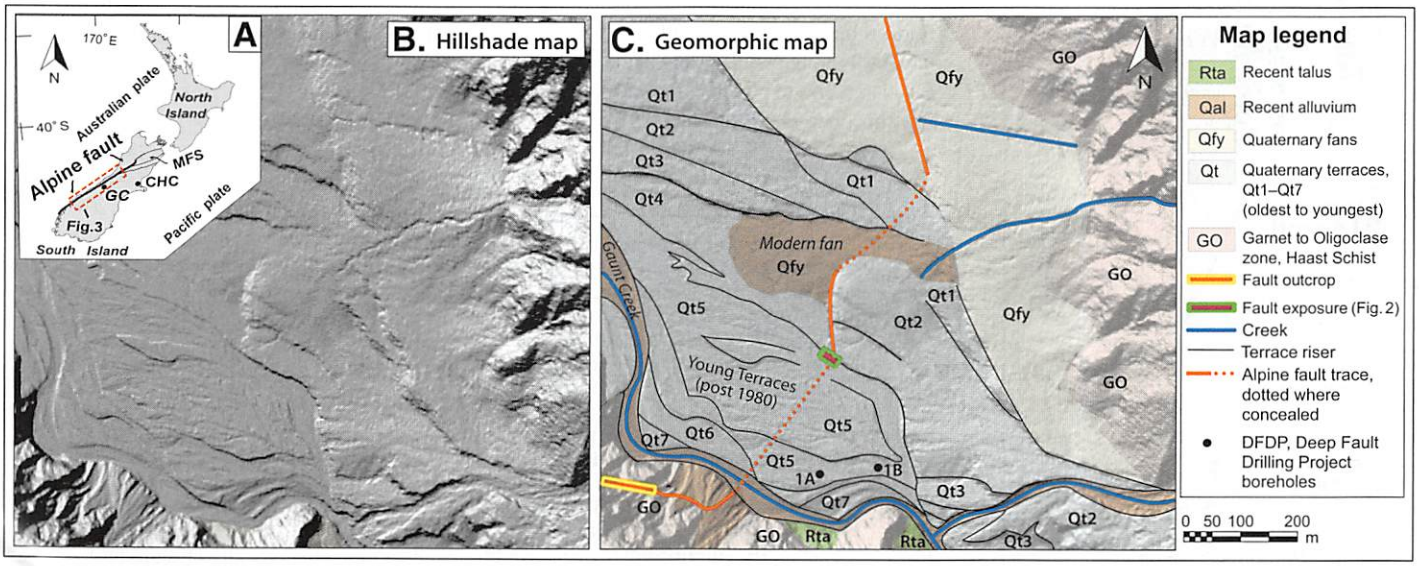

Figure 1. A: Alpine fault map on South Island of New Zealand. CHC—Christchurch, GC—Gaunt Creek, MFS—Marlborough fault system, red box—location of Figure 3. B: Uninterpreted 2 m lidar hillshade from Gaunt Creek. C: Mapping and interpretations.

---

*E-mail: gregory.depascale@pg.canterbury.ac.nz.

GEOLOGY, September 2012; v. 40; no. 9; p. 791–794; Data Repository item 2012225 | doi:10.1130/G33363.1 | Published online 29 June 2012

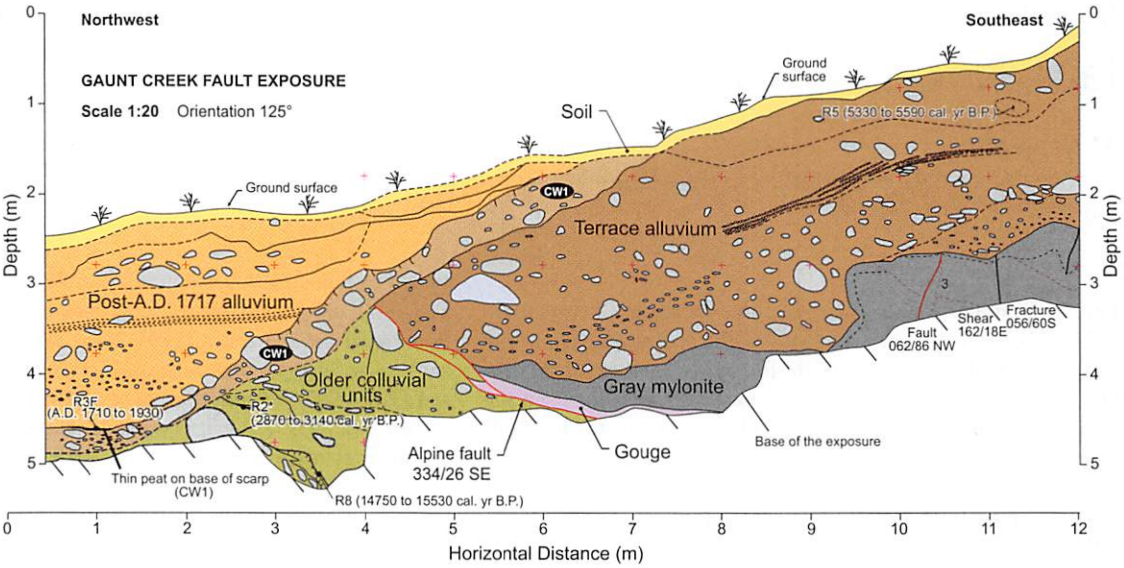

Figure 2. Log of Alpine fault exposure from Gaunt Creek (South Island, New Zealand) with radiocarbon ages (^{14}C; cal.—calibrated) and seven generalized units: mylonite bedrock, fault gouge, faulted colluvium, terrace alluvium, most recent fault scarp (CW1), post–A.D. 1717 alluvium, and the modern forest floor (soil); Alpine fault is shown in red. (See footnote 1 for the full log.)

for the fault's southern, central, and northern sections are 23 ± 1 mm yr^{-1}, 27 ± 5 mm yr^{-1}, and 14 ± 2 mm yr^{-1}, respectively (Sutherland et al., 2006; Norris and Cooper, 2001; Langridge et al., 2010). The onshore southern section extends at least ~130 km from near Milford Sound to Haast, shows primarily strike-slip motion (Cooper and Norris, 1995), and likely continues offshore south of Milford Sound (Barnes, 2009). The ~200-km-long central section extends from the Haast River to the Kokatahi River, bounds the western edge of the Southern Alps, has the highest strike-slip (27 ± 5 mm yr^{-1}) and dip-slip (8–12 mm yr^{-1}) rates, and is associated with the highest summits and overall elevation in the Southern Alps (Norris and Cooper, 2001; Little et al., 2005). Several high-slip-rate faults (e.g., Hope, Kelly) splay off the northern end of the central section, transferring plate motion to the Marlborough fault system (Van Dissen and Yeats, 1991; Langridge and Berryman, 2005). The central fault has the highest slip rate because a high proportion of the plate-boundary deformation across the South Island is accommodated by the fault, while deformation is partitioned on to other subparallel structures along the Marlborough fault system in the north (MFS, Fig. 1) and on to structures in the south, reducing slip rates along the fault in these sections (Norris and Cooper, 2001). The central section is also associated with high vertical exhumation rates, from 6 to 12 mm yr^{-1} based on geologic records (Little et al., 2005; Toy et al., 2010), and vertical deformation rates of ~5 mm yr^{-1} based on GPS data (Beavan et al., 2010).

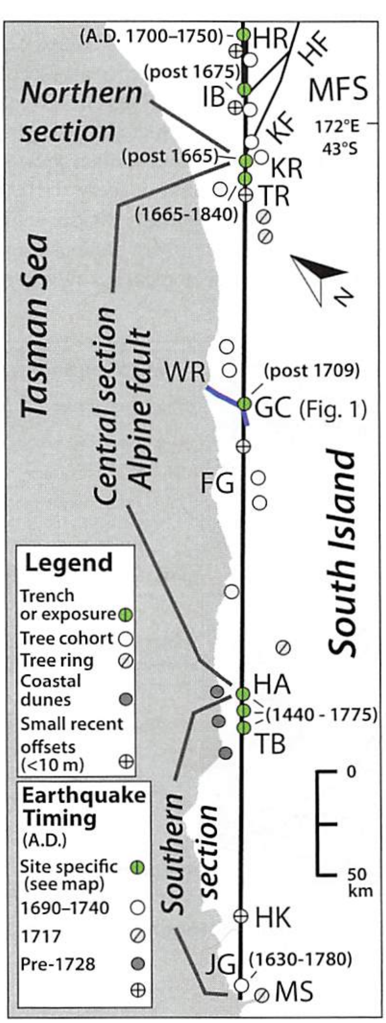

Figure 3. Map showing summary of on-fault (trench and exposure mapping) and off-fault, tree cohort (trees that simultaneously colonize surface post-disturbance), tree rings, and coastal progradation and dune formation studies showing A.D. 1717 earthquake along onshore Alpine fault (South Island, New Zealand). Data are from this study, Berryman et al. (2012), Sutherland and Norris (1995), Langridge (unpublished data), Wells et al. (1999), Wells and Goff (2007), and Yetton (2000). North to south on map: HR—Haupiri River, HF—Hope fault, MFS—Marlborough fault system, IB—Inchbonnie, KF—Kelly fault, KR—Kokatahi River, TR—Toaroha River, WR—Waitangitaona River, GC—Gaunt Creek, FG—Fox Glacier, HA—Haast, TB—Turnbull River, HK—Hokuri Creek, JG—John O'Groats, MS—Milford Sound.

Along most of its onshore length, the Alpine fault is strongly expressed as a linear, N055°E striking geomorphic lineament that divides the hanging-wall Southern Alps from the West Coast coastal plain. High relief (as much as 2000 m at the range front), dense rainforest, and high precipitation (9–14 m yr^{-1} in the Southern Alps) make both field and remotely sensed mapping difficult. Fluvial and landslide activity have overprinted the tectonic geomorphology, obscuring fault traces that formed during recent surface ruptures. Because of these challenges, there is a 200 km on-fault paleoseismicity data gap between the Haast and Toaroha Rivers.

We focused our investigations around Gaunt Creek (Fig. 1), a tributary of the Waitangitaona River, and a key site for the characterization of slip rates, fault rock sequences, and floodplain geomorphology (e.g., Cooper and Norris, 1994; Davies and Korup, 2007; Toy et al., 2010). The Alpine fault crops out on the southern side of Gaunt Creek; the outcrop is almost 700 m long and >100 m high, with mylonitized schist overthrusting late Pleistocene gravels and mylonite debris (Cooper and Norris, 1994). Adjacent to our field site, the Deep Fault Drilling Project (DFDP-1) boreholes intercepted the fault in 2011 (R. Sutherland, 2011, personal commun.). Aerial photos show that Gaunt Creek floods frequently, most recently in the 1980s (Davies and Korup, 2007), in response to precipitation and landsliding, which locally obscure fault traces.

METHODS

We mapped geological and geomorphic features using a 2 m digital elevation model (DEM) generated from airborne light detection and ranging (lidar) data (Fig. 1), and revised previous mapping from the site (Cooper and Norris, 1994). Although the area is covered by dense rainforest, the lidar data enabled us to map recent stream channels, alluvial fans, talus deposits, fluvial risers, seven different terrace surfaces (Qt1–Qt7), and faults (Fig. 1), which we validated by field checking. We targeted for field investigation a 300-m-long linear fault scarp along the northern end of the Gaunt Creek terraces, mapped the north-northwest–striking scarp in the field, and tracked it to where it intersects a subvertical terrace riser striking 125° (oblique to the fault scarp). The scarp trends northward from the terrace riser through rainforest as a 2–10-m-high, ~20°–45° west-facing scarp, and we excavated an exposure across it at the riser (Fig. 1).

RESULTS

We exposed faulted bedrock, alluvium, and colluvium buried by as much as 2.4 m of scarp-derived colluvium and alluvium, and post-MRE deposits (Fig. 2; see the GSA Data Repository[1] for the entire fault exposure log). The principal fault zone strikes north-northwest and dips southeast (334/26 SE); hanging-wall mylonites and cataclasites with fault gouge at the base of the bedrock are thrust over unconsolidated alluvium and colluvial debris on the footwall. On the hanging wall, mylonite bedrock is cut by a strath surface and overlain by a folded cobble- to boulder-sized clast-supported alluvium. Attitudes within the mylonites and cataclasites are consistent with the low-angle overthrusting observed in the gouge zone. We identified a minimum of three colluvial deposits in fault contact with the terrace alluvium and bedrock exposed in the hanging wall. Colluvium CW1 armors the scarp, overlies the principal fault plane, and is unfaulted. Below CW1, the fault is characterized by a 5–50-cm-thick zone of light bluish-gray, high-plasticity clay fault gouge with gravel inclusions forming a discrete contact zone between the terrace alluvium and older colluvial units (e.g., CW2).

Results from radiocarbon dating allow us to further interpret the complex stratigraphic and faulting history of the Alpine fault at Gaunt Creek (Table 1). A peat that formed on top of CW1 at the base of the buried scarp (sample R3F) yielded a 2σ calibrated (cal) age range of A.D. 1710–1930. Soil formed into the top of the alluvial terrace deposits (sample R5) in the hanging-wall block is 5330–5590 cal ^{14}C yr B.P. Two additional peat layers (samples R2* and R8) formed on older colluvial deposits, which are now below the fault plane, yielded 2σ calibrated ages of 2870–3140 cal ^{14}C yr B.P. and 14,750–15,530 cal ^{14}C yr B.P., respectively.

DISCUSSION

New lidar data permitted discovery of a north-striking scarp, the main trace of the Alpine fault, north of the young Gaunt Creek terraces (Qt5–Qt7), which locally obscure the surface trace. We excavated an exposure of the scarp, and documented a thrust fault with as much as 50 cm of clay fault gouge. During the MRE, coseismic uplift generated a colluvial deposit (CW1) that stabilized the fault scarp, allowing a weak soil and peat to form on the scarp. Because the footwall block was downthrown during the MRE and previous ruptures, 2.4 m of post-MRE bluish-gray alluvium derived from Gaunt Creek and its tributaries (Figs. 1 and 2) onlapped the fault while burying CW1 (including the peat we dated) and portions of the scarp, a process described by many others (e.g., see Carver and McCalpin, 1996). The stratigraphy in our exposure (Fig. 2), combined with radiocarbon dating (Table 1), indicates a history of repeated late Holocene movements, including a post–A.D. 1709 surface rupture that juxtaposed a 5 ka terrace against colluvium. The ages of the faulted colluvial deposits on the footwall that range from 2870 to 15,530 cal ^{14}C yr B.P. are likely related to prehistoric Alpine fault earthquakes. We interpret these combined observations as evidence for the A.D. 1717 rupture, and thus provide the first on-fault evidence from the high vertical deformation zone along the central Alpine fault for this postulated event. Previously, only off-fault information about the 1717 earthquake was available along the fault between the Haast area (Berryman et al., 2012) and the Toaroha River (Wells et al., 1999; Yetton, 2000), which are ~200 km apart; there were no on-fault data to support the hypothesis of a single rupture through both locations. This work also provides the first documentation of MRE thrust motion along the fault, with dominantly low-angle thrusting on a north-northwest–striking fault and consistent with the overall plate motion vector of 071° in the central South Island (DeMets et al., 1994). In addition, the strike of the thrust we document here (334°) deviates from the regional strike of the fault (055°); this supports fault partitioning models developed by Norris and Cooper (1997).

We compiled all reported on-fault and off-fault paleoseismic records for an A.D. 1717 event on the Alpine fault and suggest that at least 380 km (linear map distance) of the onshore fault ruptured, from Milford Sound to the Haupiri River (Fig. 3). Prior to this study, the 1717 event was documented in the north from on-fault trenching near the Toaroha River, Inchbonnie, and the Haupiri River, the northern terminus of the 1717 MRE (Wells et al., 1999; Yetton, 2000; our unpublished data [Langridge]), suggesting a minimum surface-rupture length of ~70 km. Our results, combined with the results of Berryman et al. (2012) from trenching near Haast, give an on-fault minimum 1717 rupture length of ~280 km between the Haupiri and Turnbull Rivers (Fig. 3). South of Turnbull, there are scant on-fault 1717 records; however, there are tree-ring chronologies near Milford Sound showing the event (Wells et al., 1999), and apparently young but undated offsets (<10 m) around Hokuri Creek (Sutherland and Norris, 1995). Based on regression equations by Hanks and Bakun (2002), which Stirling et al. (2012)

TABLE 1. RESULTS FROM RADIOCARBON DATING FROM GAUNT CREEK FAULT EXPOSURE

Sample number	Exposure unit	NZA laboratory number	δ^{13}C	Radiocarbon age (^{14}C yr B.P.)	Calibrated age 2σ (cal yr B.P. or calendar yr A.D.)		Probability for each 2σ range (%)		Material and significance
GCT-R2*	Older colluvial unit	36168	–26.5	2917 ± 30	2870–3100 cal yr B.P.	3130–3140 cal yr B.P.	94.3	0.6	Peat found in older colluvial wedge below fault plane. Dates age of paleo-earthquake on the fault?
GCT-R5	Alluvial terrace	36169	–27.8	4823 ± 30	5330–5370 cal yr B.P	5460–5590 cal yr B.P.	10.3	84.8	Peat found in alluvium of alluvial terrace. Dates the age of the terrace.
GCT-R8	Older colluvial unit	36205	–30.4	12731 ± 45	14750–15530 cal yr B.P.		95.0		Peat at base of trench below fault plane. Dates age of a paleo-earthquake on the fault?
GCT-R3F	Top of CW1	36252	–24.3	115 ± 15	A.D. 1710–1720, 1810–1840, 1850–1870, 1880–1930		7.6 5.4	28.3 53.5	Peat growing at the base of the fault scarp postdates the most recent event. Surface rupture at this location post–A.D. 1709.

Note: NZA—Rafter Radiocarbon Laboratory; B.P.—before present.

---

[1] GSA Data Repository item 2012225, detailed fault exposure photographs and log from the new Alpine fault exposure site at Gaunt Creek, New Zealand, is available online at www.geosociety.org/pubs/ft2012.htm, or on request from editing@geosociety.org or Documents Secretary, GSA, P.O. Box 9140, Boulder, CO 80301, USA.

determined best models the fault, a 380 km rupture length coupled with a seismogenic depth of 12 km (Wallace et al., 2007; Beavan et al., 2010) is equivalent to a moment magnitude of M_w 8.1 with uncertainties (based on fault geometry) of $M_w \pm 0.1$. Ultimately, the southern termination of the 1717 rupture is unknown; however, if portions of the offshore Alpine fault mapped by Barnes (2009) south of Milford Sound ruptured with the onshore portion, the 1717 earthquake was larger than the magnitude calculated here. Our analysis suggests that a great earthquake occurred on the Alpine fault in A.D. 1717, with a long surface rupture (≥380 km), displacements of as much as 10 m (Berryman et al., 2012), and up to M_w 8.2, making this similar to other major strike-slip earthquakes (e.g., the A.D. 1906 San Andreas, California, earthquake, or the 2001 Kokoxili, Tibet, earthquake). The absence of any significant historical event along the fault, combined with data from the central section showing a great (M8+) earthquake in 1717, serves as a reminder that the fault remains the most significant seismic hazard on the South Island. After the Canterbury earthquakes of 2010–2012, incorporating updated Alpine fault paleoseismicity data is critical to promote infrastructure resilience throughout New Zealand during future seismic events and great earthquakes.

ACKNOWLEDGMENTS

We thank P. Falk, A. Zajac, T. Hamilton, and V. Ewing for field-work assistance, Tim Davies, Mark Quigley, and two anonymous reviewers for useful improvements to this paper, and Carolyn Mosher for help with graphics. De Pascale is supported by the University of Canterbury's Mason Trust and Hari-Hari field station, a New Zealand International Doctoral Research Scholarship from Education New Zealand, and a Wellman Award by the Geoscience Society of New Zealand. Funding was provided to Langridge by the GNS Science FRST PLT (Plate Tectonics of New Zealand) program. We thank Rupert Sutherland for his Alpine fault insight, Mark Stirling for earthquake scaling discussions, and the New Zealand Department of Conservation for site access.

REFERENCES CITED

Adams, J., 1980, Paleoseismicity of the Alpine fault seismic gap, New Zealand: Geology, v. 8, p. 72–76, doi:10.1130/0091-7613(1980)8<72:POTAFS>2.0.CO;2.

Barnes, P.M., 2009, Postglacial (after 20 ka) dextral slip rate of the offshore Alpine fault, New Zealand: Geology, v. 37, p. 3–6, doi:10.1130/G24764A.1.

Beavan, J., Denys, P., Denham, M., Hager, B., Herring, T., and Molnar, P., 2010, Distribution of present-day vertical deformation across the Southern Alps, New Zealand, from 10 years of GPS data: Geophysical Research Letters, v. 37, L16305, doi:10.1029/2010GL044165.

Berryman, K.R., Beanland, S., Cooper, A.F., Cutten, H.N., Norris, R.J., and Wood, P.R., 1992, The Alpine Fault, New Zealand: Variation in Quaternary structural style and geomorphic expression: Annales Tectonicae, v. 6, p. 126–163.

Berryman, K., Cooper, A., Norris, N., Villamor, P., Sutherland, R., Wright, T., Schermer, E., Langridge, R., and Baisi, G., 2012, Late Holocene rupture history of the Alpine fault in South Westland, New Zealand: Seismological Society of America Bulletin, v. 102, p. 620–638, doi:10.1785/0120110177.

Bull, W.B., 1996, Prehistorical earthquakes on the Alpine fault, New Zealand: Journal of Geophysical Research, v. 101, no. B3, p. 6037–6050, doi:10.1029/95JB03062.

Carver, G.A., and McCalpin, J.P., 1996, Paleoseismology of compressional tectonic environments, *in* McCalpin, J.P., ed., Paleoseismology: San Diego, California, Academic Press, p. 183–270.

Cooper, A.F., and Norris, R.J., 1994, Anatomy, structural evolution, and slip rate of a plate-boundary thrust: The Alpine fault at Gaunt Creek, Westland, New Zealand: Geological Society of America Bulletin, v. 106, p. 627–633, doi:10.1130/0016-7606(1994)106<0627:ASEASR>2.3.CO;2.

Cooper, A.F., and Norris, R.J., 1995, Displacement of the Alpine Fault at Haast River, South Westland, New Zealand: New Zealand Journal of Geology and Geophysics, v. 38, p. 509–514, doi:10.1080/00288306.1995.9514677.

Cubrinovski, M., and 19 others, 2011, Geotechnical Aspects of the 22 February 2011 Christchurch Earthquake: New Zealand Society for Earthquake Engineering Bulletin, v. 44, p. 205–226.

Davies, T.R., and Korup, O., 2007, Persistent alluvial fanhead trenching resulting from large, infrequent sediment inputs: Earth Surface Processes and Landforms, v. 32, p. 725–742, doi:10.1002/esp.1410.

DeMets, C., Gordon, R.G., Argus, D.F., and Stein, S., 1994, Effect of recent revisions to the geomagnetic reversal time scale on estimates of current plate motions: Geophysical Research Letters, v. 21, p. 2191–2194, doi:10.1029/94GL02118.

Hanks, T.C., and Bakun, W.H., 2002, A bilinear source-scaling model for M-log A observations of continental earthquakes: Bulletin of the Seismological Society of America, v. 92, p. 1841–1846, doi:10.1785/0120010148.

Langridge, R.M., and Berryman, K.R., 2005, Morphology and slip rates of the Hurunui section of the Hope Fault, South Island, New Zealand: New Zealand Journal of Geology and Geophysics, v. 48, p. 43–57, doi:10.1080/00288306.2005.9515097.

Langridge, R.M., Villamor, P., Basili, R., Almond, P., Martinez-Diaz, J.J., and Canora, C., 2010, Revised slip rates for the Alpine fault at Inchbonnie: Implications for plate boundary kinematics of South Island, New Zealand: Lithosphere, v. 2, p. 139–152, doi:10.1130/L88.1.

Little, T.A., Cox, S., Vry, J.K., and Batt, G., 2005, Variations in exhumation level and uplift rate along the oblique-slip Alpine fault, central Southern Alps, New Zealand: Geological Society of America Bulletin, v. 117, p. 707–723, doi:10.1130/B25500.1.

Norris, R.J., and Cooper, A.F., 1997, Erosional control on the structural evolution of a transpressional thrust complex on the Alpine fault, New Zealand: Journal of Structural Geology, v. 19, p. 1323–1342, doi:10.1016/S0191-8141(97)00036-9.

Norris, R.J., and Cooper, A.F., 2001, Late Quaternary slip rates and slip partitioning on the Alpine fault, New Zealand: Journal of Structural Geology, v. 23, p. 507–520, doi:10.1016/S0191-8141(00)00122-X.

Quigley, M., Van Dissen, R., Litchfield, N., Villamor, P., Duffy, B., Barrell, D., Furlong, K., Stahl, T., Bilderback, E., and Noble, D., 2012, Surface rupture during the 2010 Mw 7.1 Darfield (Canterbury, New Zealand) earthquake: Implications for fault rupture dynamics and seismic-hazard analysis: Geology, v. 40, p. 55–58, doi:10.1130/G32528.1.

Rhoades, D.A., and Van Dissen, R.J., 2003, Estimates of the time-varying hazard of rupture of the Alpine Fault, New Zealand, allowing for uncertainties: New Zealand Journal of Geology and Geophysics, v. 46, p. 479–488, doi:10.1080/00288306.2003.9515023.

Stirling, M.W., and 20 others, 2012, National Seismic Hazard Model for New Zealand:

2010 Update: Bulletin of the Seismological Society of America (in press).

Sutherland, R., and Norris, R.J., 1995, Late Quaternary displacement rate, paleoseismicity, and geomorphic evolution of the Alpine Fault: Evidence from Hokuri Creek, South Westland, New Zealand: New Zealand Journal of Geology and Geophysics, v. 38, p. 419–430, doi:10.1080/00288306.1995.9514669.

Sutherland, R., Berryman, K., and Norris, R., 2006, Quaternary slip rate and geomorphology of the Alpine fault: Implications for kinematics and seismic hazard in southwest New Zealand: Geological Society of America Bulletin, v. 118, p. 464–474, doi:10.1130/B25627.1.

Sutherland, R., and 18 others, 2007, Do great earthquakes occur on the Alpine fault in central South Island, New Zealand?, *in* Okaya, D., et al., eds., A continental plate boundary: Tectonics at South Island, New Zealand: American Geophysical Union Geophysical Monograph 175, p. 235–251, doi:10.1029/175GM12.

Toy, V.G., Craw, D., Cooper, A.F., and Norris, R.J., 2010, Thermal regime in the central Alpine Fault zone, New Zealand: Constraints from microstructures, biotite chemistry and fluid inclusion data: Tectonophysics, v. 485, p. 178–192, doi:10.1016/j.tecto.2009.12.013.

Van Dissen, R.J., and Yeats, R.S., 1991, Hope fault, Jordan thrust, and uplift of the Seaward Kaikoura Range, New Zealand: Geology, v. 19, p. 393–396, doi:10.1130/0091-7613(1991)019<0393:HFJTAU>2.3.CO;2.

Walcott, R.I., 1978, Present tectonics and late Cenozoic evolution of New Zealand: Royal Astronomical Society Geophysical Journal, v. 52, p. 137–164, doi:10.1111/j.1365-246X.1978.tb04225.x.

Wallace, L.M., Beavan, J., McCaffrey, R., Berrymany, K., and Denys, P., 2007, Balancing the plate motion budget in the South Island, New Zealand using GPS, geological and seismological data: Geophysical Journal International, v. 168, p. 332–352, doi:10.1111/j.1365-246X.2006.03183.x

Wellman, H.W., 1953, Data for the study of Recent and late Pleistocene faulting in the South Island of New Zealand: New Zealand Journal of Science and Technology, v. 34B, p. 270–288.

Wells, A., and Goff, J., 2007, Coastal dunes in Westland, New Zealand, provide a record of paleoseismic activity on the Alpine fault: Geology, v. 35, p. 731–734, doi:10.1130/G23554A.1.

Wells, A., Yetton, M.D., Duncan, R.P., and Stewart, G.H., 1999, Prehistoric dates of the most recent Alpine fault earthquakes, New Zealand: Geology, v. 27, p. 995–998, doi:10.1130/0091-7613(1999)027<0995:PDOTMR>2.3.CO;2.

Yetton, M.D., 2000, The probability and consequences of the next Alpine Fault earthquake, South Island, New Zealand [Ph.D. thesis]: Christchurch, New Zealand, University of Canterbury, 312 p.

Manuscript received 1 March 2012
Revised manuscript received 23 March 2012
Manuscript accepted 24 March 2012

Printed in USA